Beijer Institute
OF ECOLOGICAL ECONOMICS

KUNGL. VETENSKAPS-AKADEMIEN
THE ROYAL SWEDISH ACADEMY OF SCIENCES

DISCUSSION PAPER

Cascading regime shifts in pollution recipients and resource systems

Beijer Discussion Paper Series No. 275

Anne-Sophie Crépin and Juan Carlos Rocha. 2021.

Beijer Institute of Ecological Economics
The Royal Swedish Academy of Sciences

Lilla Frescativägen 4A
Stockholm

+46 8 673 95 00
beijer@beijer.kva.se

www.beijer.kva.se

Cascading regime shifts in pollution recipients and resource systems

Anne-Sophie Crépin*and Juan Carlos Rocha†

June 21, 2021

*The Beijer Institute of Ecological Economics, the Royal Swedish Academy of Sciences, Lilla Frescativägen 4A, box 50005, 10405 Stockholm Sweden and the Stockholm Resilience Centre, Stockholm University, 10691 Stockholm Sweden, ORCID: 0000-0002-7370-2973

†The Stockholm Resilience Centre, Stockholm University, 10691 Stockholm Sweden, ORCID:0000-0003-2322-5459

Abstract

Ecosystems can undergo regime shifts − large, abrupt and persistent changes in their structure and function. These regime shifts can interact with each other creating cascading effects. We explore potential characteristics of such interactions and their outcomes. We focus on two types of systems where regime shifts can substantially influence human welfare and livelihoods: pollution recipients, such as the atmosphere and water bodies, and renewable resources, such as wild animal stocks. We set up a dynamic modeling framework where patches of either pollution recipients or resource producing systems interact with each other. We identify clear mechanisms, through which cascading effects can either increase the probability of a shift in a particular patch or decrease it. We also investigate the conditions for optimal control of such systems. We show that spatial dispersion can trigger regime shifts in controlled and uncontrolled systems compared to systems without dispersion.

Keywords— Cascading effects; Regime shifts; Pollution; Natural resources

1 Introduction

Ecosystem regime shifts are abrupt, persistent, and substantial changes in a system's structure and function that can come as surprises [Biggs et al., 2012a]. Such abrupt ecosystem changes are pervasive phenomena with sometimes substantial welfare implications for the people enjoying services from these ecosystems [Rocha et al., 2015]. These phenomena are being widely studied to assess the extent of their implications on human well-being in general and economic incentives in particular [Horan et al., 2011, Crépin et al., 2012, Li et al., 2018]. While most studies of regime shifts have focused on what happens in one particular system, empirical evidence indicates that regime shifts can spread between different systems and in multiple ways [Anderies et al., 2006, Peters et al., 2007, Mueller et al., 2009, Rocha et al., 2015]. Scientists have studied these phenomena using network theory [Rocha et al., 2018] and multiple modelling frameworks [Kinzig et al., 2006, Krönke et al., 2019]). Previous studies have focused on spatial or organisational scales [Kinzig et al., 2006] and identifying some mechanisms for regimes shifts to spread between different systems [Rocha et al., 2018].

This paper aims to further the understanding of cascading regime shifts in contexts relevant for ecosystem services and their support of human well being. While there is now an increasing amount of empirical data on regime shifts (www.regimeshifts.org), this data is rarely of a resolution that would allow for a detailed empirical analysis of the particular mechanisms involved when those systems are connected. Instead we resort to modelling and model experiments to investigate possible mechanisms that could underlie cascading regime shifts. Hence we aim to develop theoretical models to study how potential regime shifts

in external systems can influence the likelihood of tipping a particular system to an alternate regime.

These questions relate to finding approaches to managing connectivity. Cascading regime shifts can only occur in a connected world and will thus depend on how different parts of this world connect with each other. The principles of resilience [Biggs et al., 2012b, 2015] include *manage connectivity* as one of the principles for managing system properties. However, the scientific literature that provide details about how to manage this connectivity is limited. Brock et al. [2020] provide an overview of the economic literature in this field. They identify various ways to incorporate spatial dimensions and transports into models. In particular space can be treated as a continuum or as a collection of discrete patches.

Here we use the latter representation of space, which is the most encountered in environmental and resource economics through metapopulation models. We believe it is a more accurate representation of the typical problems we have in mind, where the spatial domain is patchy and those patches can be connected in different ways e.g. via water transports between different water bodies or species' migration to other marine or terrestrial territories. Dispersion is modelled as a system of ordinary differential equations (ODE).

An extensive bioeconomic literature focusing mostly on aquatic systems incorporates spatial dispersion in an optimal management context [Sanchirico and Wilen, 1999, Wilen, 2007, Smith et al., 2009, Kroetz and Sanchirico, 2015]. In the atmosphere, the "acid rain game" literature also uses a similar approach [Mäler, 1989, Kaitala et al., 1992, Mäler and De Zeeuw, 1998, Nagase and Silva, 2007],

where suplhur emissions from emitting regions is transported in the atmosphere to other regions where it falls as acid rain. This literature typically discards the possibility of regime shifts and thus also the possibility that they might spread between different areas.

The literature on earth system dynamics contributes several recent models with possibilities of cascading shifts [Klose et al., 2020, Wunderling et al., 2020a,b]. These models consist of general dynamic equations, which represent potential connections between climate tipping elements. They find that minimal geometrical shapes in the network structure such as triangles (network motifs) can destabilize networked systems, and high clustering (or the proportion of closed paths) can amplify cascading effects. These two findings mean that the higher the number of connections, the higher the probability that diffusion processes will amplify cascades. Modeling work on tipping cascades has shown that, in small systems, the tipping of one element can jump intermediate systems and push an end of chain system over [Brummitt et al., 2015]. In addition, early warning signals applied to coupled climate systems render poor detection of cascading effects [Dekker et al., 2018]. However these results are difficult to interpret in the context of resource or pollution management typically studied in environmental and resource economics.

Here we develop a framework that will allow us to study the potential for tipping cascades between different patches of interest for human well-being. We want to focus particularly on the studied system's capacity to provide critical provisioning of ecosystem services in the event of cascading regime shifts. We also aim to link to existing economic literature related to natural resource management with potential regime shifts, which does not consider spacial dispersion [Carpenter

et al., 1999, Crépin, 2002, 2003, 2007, Brock and Starrett, 2003, Mäler et al., 2003, Wagener, 2003].

We propose to focus on two typical and iconic systems as the basic nodes of our world of connected systems: pollution recipients and resource production systems. Both types of systems are widely studied in the environmental and resource economics literature and using bioeconomic modelling. The pollution recipient can shift between a clean and a polluted regime. Iconic case studies for this system type would be nutrients in lakes, rivers or seas [Brock and Starrett, 2003, Mäler et al., 2003, Wagener, 2003] or atmospheric pollution such as CO_2 in the atmosphere [Crépin and Nævdal, 2019]. The resource system is featured as a resource with logistic growth [Verhulst, 1838], which can be predated (Holling type III predation, [Holling, 1959]), such as a fish stock, which can then exist in an abundant regime or an alternate persistent low stock regime [Crépin, 2002, 2007]. Most of the regime shifts types documented in the regime shift database (27 out of 30) represent either resource production systems, pollution systems or both (6.1). This illustrates that the type of systems we consider here are relevant for society and that regime shifts can be pervasive in those systems.

First we present the two models of resource and pollution stock in more detail (2) before studying the implication of having systems of multiple connected patches of either pollution or resource systems. The connection in each of these systems consists of flows of pollution or species (depending on the type of system) that move between different patches (3). We then investigate the control of such connected system and derive golden rules for pollution regulation and resource exploitation in a context of multiple connected patches that can shift between alternative regimes

(4). Finally we discuss the implications of these findings for management (5).

2 Modelling framework

Here we introduce the details of a pollution model (2.1) and a resource model (2.2). Consider a set of n patches, each patch $i \in \{1, ...n\}$ consists of either a pollution recipient or a resource system.

2.1 Pollution

Here we use a general form of the lake model [Mäler et al., 2003, Wagener, 2003]. Let x_i denote a stock of pollutant in patch i. Let u_i denote the load of pollutants from human activities to patch i and s_i the internal rate of loss —in a lake it can for example be the nutrients that sediment or are absorbed in biomass. For low nutrient levels, the release is minimal but above some threshold z_i, the system flips to a high release level. The term v_i is the maximum level of internal nutrient release and the parameter α_i indicates the sharpness of the shift. The highest this parameter is, the sharpest the shift between a low and a high level of internal release of nutrient. For values close to 1 the shift is smooth. The term $v_i \frac{x_i^{\alpha_i}}{z_i^{\alpha_i}+x_i^{\alpha_i}}$ represents nutrient release within the recipient —e.g. from the bottom sediment of a lake for water pollution or from the ocean or soil for atmospheric pollution like methane from melting permafrost. For all $i \in \{1, ...n\}$:

$$\frac{dx_i}{dt} = u_i - s_i x_i + v_i \frac{x_i^{\alpha_i}}{z_i^{\alpha_i} + x_i^{\alpha_i}}. \tag{1}$$

This system exhibits two different regimes depending on the size of the net inflow to the system, $u_i - s_i x_i$ compared to the size of the internal release, $v_i \frac{x_i^{\alpha_i}}{z_i^{\alpha_i} + y_i^{\alpha_i}}$. A high net inflow in equilibrium is associated with a higher internal release —because x_i must then be larger in equilibrium—and thus a higher risk of reaching a high pollution regime compared to situations of low net inflow. The green curves in figure 1 represent the internal release, while the blue straight lines represent the net inflow. For low pollution inflow, there could be only one low pollution equilibrium, while for high pollution inflow there would be a unique high pollution equilibrium. When pollution inflow is intermediate, multiple equilibria can occur and the outcome depends on initial conditions [Mäler et al., 2003]. Note that the three sub-figures in figure 1 all represent the same case without dispersion with three possible equilibria (where the green curves and blue lines intersect). The left- and right-hand side equilibria are stable. They represent a low, respectively a high nutrient regime, while the middle equilibrium is unstable.

2.2 Resource

Let y_i denote the stock of an ecosystem resource in patch i. The resource has carrying capacity k_i, and intrinsic growth rate r_i. Let some parameter c_i represent the availability of refuges for example for protection against predators in patch i. Let q_i denote the rate of half-saturation biomass for predators i.e. the threshold population level above which predation shifts from a low to a high level —the location of the inflection point of an S-shape curve. Let β_i denote a curvature parameter. The higher the value of β_i, the steeper the shift between a low and a high level of predation. The first term in equation 2 represents a logistic growth

[Verhulst, 1838], the second term is a Holling type III predation rate [Holling, 1959].

$$\frac{dy_i}{dt} = r_i y_i \left(1 - \frac{y_i}{k_i}\right) - c_i \frac{y_i^{\beta_i}}{q_i^{\beta_i} + y_i^{\beta_i}}. \tag{2}$$

Here again, this system exhibits two different regimes depending on the relative size of the logistic growth term, $r_i y_i \left(1 - \frac{y_i}{k_i}\right)$ (blue curves in figure 2) compared to the availability of refuges, $c_i \frac{y_i^{\beta_i}}{q_i^{\beta_i} + y_i^{\beta_i}}$ (green curves in figure 2). The blue and green curves in figure 2 illustrate how these two functions relate to each other. Here again, the four sub-figures in figure 2 all represent the same case without dispersion with three possible interior equilibria (where the green curves and blue lines intersect).[1] The left- and right-hand side interior equilibria are stable. They represent a low, respectively a high resource stock regime, while the middle equilibrium is unstable.

3 Cascading effects between similar systems

Multiple systems of the two basic types considered could be connected with each other in many different ways. Here, we systematically investigate the two cases when the connected systems are of similar type (either resource or pollution). We model these interactions as a flow of stock between the different systems. The analysis of these two cases developed in sections 3.1 and 3.2 provides graphical analytical results.

[1] Note that sub-figure c uses different scales on the axes to incorporate the whole graph of the red curve, which will be discussed in section 3.2.

3.1 Cascading shifts between pollution systems

Let the term δ_{ij} represent the coefficient of pollution dispersion from patch i to some other patch j. Note that in general, $\delta_{ij} \neq \delta_{ji}$. The term $\delta_{ij}x_i - \delta_{ji}x_j$ represents the net dispersion between two patches i and j. If $\delta_{ij}x_i - \delta_{ji}x_j > 0$, patch i will be a source, while patch j is a recipient. If the difference is negative, the opposite holds true. For all i and j in $\{1, ...n\}$, the pollution model with dispersion becomes:

$$\frac{dy_i}{dt} = u_i - s_i x_i + v_i \frac{x_i^{\alpha_i}}{z_i^{\alpha_i} + x_i^{\alpha_i}} - \sum_{j \neq i} (\delta_{ij}x_i - \delta_{ji}x_j). \tag{3}$$

Using this modelling framework we can assess the potential for cascading regime shifts between systems of similar types by studying the impact of the dispersion term on system stability. We analyse and illustrate this graphically by comparing the diagrams that illustrate equilibrium points of equations 1 and 3 for pollution systems.

It is possible to simplify the analysis even more by transforming the equations so as to minimize the number of key parameters – see appendix 6.2. Let r denote the time difference between t and τ, let $X_i = \frac{x_i}{z_i}$, $\frac{dt}{d\tau} = \frac{1}{r}$, $U_i = \frac{u_i}{rz_i}$, $S_i = \frac{S_i}{r}$ $V_i = \frac{v_i}{rz_i}$, $Z_{ij} = \frac{\delta_{ji}z_j}{\delta_{ij}z_i}$ and $\Delta_{ij} = \frac{\delta_{ij}}{r}$, we obtain:

$$\frac{dX_i}{d\tau} = U_i - S_i X_i + V_i \frac{X_i^{\alpha_i}}{1 + X_i^{\alpha_i}} + \sum_{j \neq i} \Delta_{ij}(Z_{ij}X_j - X_i) \tag{4}$$

.

Equation 4 has the same topological characteristics as equation 3. Setting $\Delta_{ij} = 0$ for all values of i and j, we obtain a model with the same topological

characteristics as equation 1, the model without dispersion. For all $i \in \{1, ..., n\}$:

$$\frac{dX_i}{d\tau} = 0 \Leftrightarrow V_i \frac{X_i^{\alpha_i}}{1 + X_i^{\alpha_i}} = S_i X_i - U_i - \sum_{j \neq i} \Delta_{ij}(Z_{ij} X_j - X_i) \tag{5}$$

The solution to equation 5 is a polynomial of degree $\alpha_i + 1$. However, the equilibria in each of the n patches can be fully characterized as the intersection between two curves in $\mathbb{R}^+$ (Figure 1). The left hand side of equation 5 is an S-shaped curve (green curves in Figure 1). Its value is 0 at the origin and it approaches V_i asymptotically as $X_i \to +\infty$. This curve has an inflection point at $(1, V_i/2)$ and the steepness of the curve depends on α_i: the higher α_i, the steepest the curve is around the inflection point and the flattest it is elsewhere. This curve remains the same whether of not there is dispersion between patches because the impacts of dispersion are fully incorporated in the right hand side of equation 5.

This right hand side can be represented by a straight line. Without dispersion (straight blue line), it goes through the points $(0, -U_i)$ and $(U_i, 0)$. With dispersion (straight red line), it goes instead through the points $(0, \Delta)$ and $\left(\frac{-\Delta}{1+\sum_{j \neq i} \Delta_{ij}}, 0\right)$ where $\Delta = -U_i - \sum_{j \neq i} \Delta_{ij} Z_{ij} X_j$. Note that $\Delta \leq -U_i$ and the slope of the right hand side is equal to $1 + \sum_{j \neq i} \Delta_{ij} \geq 1$. This means that the straight line with dispersion is always steeper than without dispersion but intersects with the vertical axis at a lower level. Thus there will be risk trade offs depending on where the straight lines intersect with each other, which occurs when $Z_{ij} X_j = X_i$ at the intersection point $(Z_{ij} X_j, Z_{ij} X_j - U_i)$. The possible intersection of a straight line with an S-shaped curve, given that $U_i > 0$, gives rise to at least one equilibrium and at most three with real values of $X_i \geq 0$.

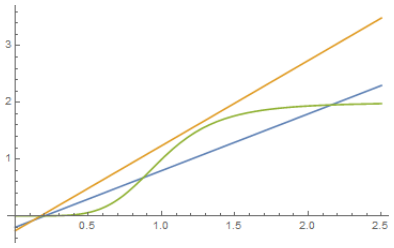

(a) $X_j = 0, 1$

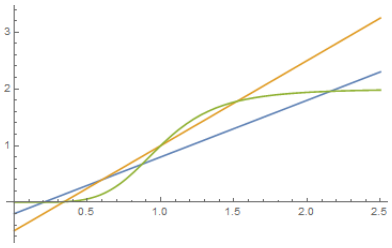

(b) $X_j = 1$

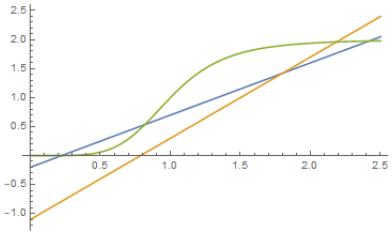

(c) $X_j = 3$

Figure 1: Graphical illustration of potential equilibria in a pollution system. The green sigmoid curve represents the internal release of pollutants, which is the same with and without dispersion. The straight lines represent the net inflow to the system without dispersion (blue) and with dispersion (orange). Figures a) b) and c) represent respectively low, intermediate and high size stocks in other patches (X_j). For simplification all other patches are lumped into patch j here. Figures drawn using Mathematica. $U_i = 0, 2; V_i = 2; s_i = 0.9; \alpha = 5; \Delta_{ij} = 0, 5; Z_i j = 0, 6$.

3.2 Cascading shifts between resource systems

Consider the resource stock model (2). Similar to section 3.1, let the dispersion parameter d_{ij} represent the dispersion rate of the resource y from patch i to patch j. It is the share of the stock y_i that moves to the patch j. The last term in equation 6 is a linear dispersion term (Murray [2001], Okubo and Levin [2013]). It shows the net dispersion between patches i and j.

$$\frac{dy_i}{dt} = r_i y_i \left(1 - \frac{y_i}{k_i}\right) - c_i \frac{y_i^{\beta_i}}{q_i^{\beta_i} + y_i^{\beta_i}} - \sum_{j \neq i} (d_{ij} y_i - d_{ji} y_j). \tag{6}$$

To facilitate comparisons between the resource systems without dispersion (2) and with dispersion (6), we transform the systems into non-dimensional forms, with a minimal number of critical parameters but the same dynamic characteristics (See Appendix 6.3). Let r denote the time difference between t and τ, $R_i = \frac{r_i}{r}$, $K_i = \frac{k_i}{q_i}$, $C_i = \frac{c_i}{r q_i}$, $Q_{ij} = \frac{d_{ji} q_j}{d_{ij} q_i}$, and $D_{ij} = \frac{d_{ij}}{r}$, we obtain the system with dispersion in non-dimensional form, which has the same topological characteristics as equation 6:

$$\frac{dY_i}{d\tau} = R_i Y_i \left(1 - \frac{Y_i}{K_i}\right) - C_i \frac{Y_i^{\beta_i}}{1 + Y_i^{\beta_i}} + \sum_{j \neq i} D_{ij} (Q_{ij} Y_j - Y_i) \tag{7}$$

Letting $D_{ij} = 0$ for all i and j provides the system without dispersion in non-dimensional form, which has the same topological characteristics as equation 2:

$$\frac{dY_i}{d\tau} = R_i Y_i \left(1 - \frac{Y_i}{K_i}\right) - C_i \frac{Y_i^{\beta_i}}{1 + Y_i^{\beta_i}} \tag{8}$$

.

Setting both equations equal to zero, we can then characterize their equilibria:

$\forall i \in \{1, ..., n\}$; $\frac{dY_i}{d\tau} = 0$ yields equation 9 without dispersion and 10 with dispersion.

$$C_i \frac{Y_i^{\beta_i}}{1 + Y_i^{\beta_i}} = R_i Y_i - \frac{R_i (Y_i)^2}{K_i} \tag{9}$$

$$C_i \frac{Y_i^{\beta_i}}{1 + Y_i^{\beta_i}} = \left(R_i - \sum_{j \neq i} D_{ij} \right) Y_i - \frac{R_i (Y_i)^2}{K_i} + \sum_{j \neq i} D_{ij} Q_{ij} Y_j \tag{10}$$

Similar to the pollution case, the equilibria can be characterised analytically in $\mathbb{R}^+$ as the intersections of the graphs of two functions. The left hand sides of equations (9) and (10) are the same and they have a similar shape to the corresponding curve in the pollution case (equation 5) except that the asymptote occurs at C_i instead of V_i, and β_i characterizes the sharpness of the curve instead of α_i.

The right hand sides of equations (9) and (10) are both concave functions but they differ between the two cases. The function without dispersion (9), has value 0 at the origin and at $Y_i = K_i$ and a maximum of $K_i/4$ at $Y_i = K_i/2$. To investigate the behaviour of the right hand side with dispersion (10), let's define some intermediate variables:

- $D \equiv \sum_{j \neq i} D_{ij} Q_{ij} Y_j$, the total inflow from other plots.
- $\bar{D} \equiv R_i - \sum_{j \neq i} D_{ij}$, the net growth of the stock (intrinsic growth minus all outflow from plot i to other plots.
- $\hat{D} \equiv \sqrt{\left(\bar{D}\right)^2 + 4 \frac{R_i}{K_i} D}$.

With dispersion, the right hand side goes through the points $(0, D)$, and $\left(\frac{K_i}{2R_i} \left(\bar{D} + \hat{D} \right), 0 \right)$ and reaches a maximum at $\left(\frac{K_i}{2R_i} \bar{D}, \frac{K_i}{4R_i} \bar{D}^2 + D \right)$

Hence we obtain the following results:

1. When the stock in plot i is zero, the stock does not grow without dispersion while it grows with D with dispersion.

2. The total carrying capacity of the resource in plot i is K_i without dispersion and $\frac{K_i}{2R_i}\left(\bar{D}+\hat{D}\right)$ with dispersion. Which of these two is larger than the other will depend on the values of D_{ij} and Q_{ij}. For relatively large values of D_{ij} and relatively low values of Q_{ij}, the carrying capacity will be larger in the plot without dispersion while for relatively low values of D_{ij} and relatively high values of Q_{ij}, the opposite holds true. This makes sense: when the outflow to other plots is large enough compared to the inflow from other plots, the plot is likely to support fewer individuals at carrying capacity.

3. The maximum stock growth occurs at lower or equal stock levels with dispersion compared to without dispersion (compare $\frac{K_i}{2}$ and $\frac{K_i\bar{D}}{2R_i}$) if and only if $R_i > \sum_{j\neq i} D_{ij}$.[2]

4. The maximum stock growth is higher with dispersion compared to without if and only if $\frac{K_i}{4R_i}\bar{D}^2 + D > \frac{K_i}{4}$. This occurs only when the total inflow from other plots and the net growth of the stock are relatively large compared to the intrinsic growth rate.

Hence we can identify different cases depending on the relative values of D and $\bar{D}$ (figure 2). For example if D is large enough (larger than $K_i \sum_{j\neq i} D_{ij}$) the orange curve (with dispersion) will always lie above the blue curve (without dispersion) –

[2]A negative $\bar{D}$ means that i patch i intrinsic growth is lower than gross outflow. For an equilibrium to occur, substantial inputs from other patches must compensate for the deficit.

figures 2a and 2c. This implies that the equilibrium, at the intersection with the green curve always implies higher stock levels with dispersion.For lower values of D than $K_i \sum_{j \neq i} D_{ij}$, the orange and blue curves intersect once when $Y_i = \frac{D}{\sum_{j \neq i} D_{ij}}$. For values of Y_i below this intersection point, the orange curve is above the blue curve and for larger values of y_i, it lies below the blue curve. Figures 2b and 2d illustrate such case. Note that the intersection point in those cases occurs for values of Y_i that are low enough to yield $\sum_{j \neq i} D_{ij}(Q_{ij}Y_j - Y_i) < 0$. These values are low compared to the carrying capacity and thus cannot be seen in the figures.

4 Controlling cascades

How can we manage this type of systems? Here we investigate the optimal control of spatially defined pollution and resource systems, where a manager can control the inflow of nutrients in pollution systems or the harvests in resource systems. This can serve as a limit case for what is possible to achieve through management. Let ρ denote the discount rate. We set up the two following general control problems for pollution and resource systems respectively.

4.1 Controlling pollution cascades

Let $P_i(X_i, U_i)$ denote the instantaneous objective in each patch i. This functions is on purpose general enough to represent many kinds of objectives. It could represent for example a profit function of a firm deciding about how much to

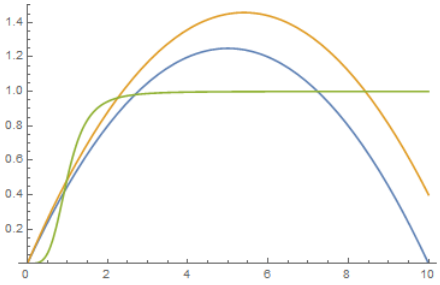

(a) $\sum_{j \neq i} D_{ij} = 0.06$; $D = 0.1$

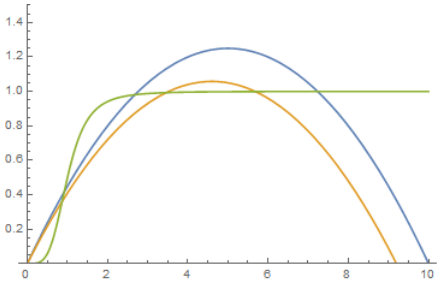

(b) $\sum_{j \neq i} D_{ij} = 0.06$; $D = 0.02$

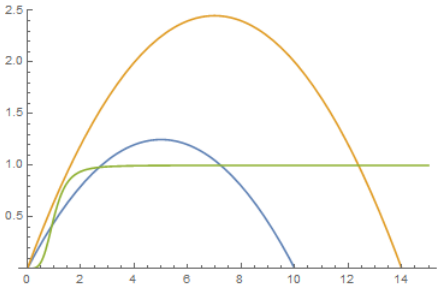

(c) $\sum_{j \neq i} D_{ij} = 0.2$; $D = 0.4$

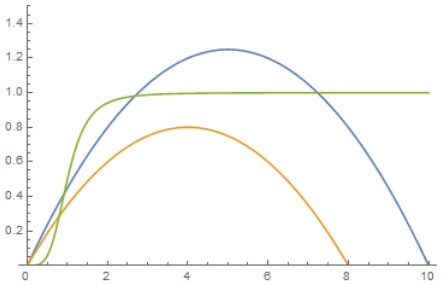

(d) $\sum_{j \neq i} D_{ij} = 0.2$; $D = 0.1$

Figure 2: Equilibria in a resource system. The curves represent the predation rate (green) and the logistic growth with (red) and without dispersion (blue). When the total inflow from other plots is high (low) compared to the outflow, the equilibrium stocks are higher (lower) with dispersion, cases a and c (b and d). The number of equilibria can even change with dispersion compared to without (c and d). All other patches than i are lumped. Figures drawn using Mathematica. $R_i = 0.5$; $K_i = 10$; $C_i = 1$; $\beta_i = 4$.

pollute or a social welfare function, which then could also include whole bundles of ecosystem services that the system studied provides.

Let X and U, respectively, denote vectors of pollution stocks $(X_i)_{i\in\{1,\dots,n\}}$ respectively pollution inflows $(U_i)_{i\in\{1,\dots,n\}}$, where pollution inflows can be controlled. We can formulate a manager's pollution problem as choosing an appropriate level of pollution inflow that optimizes the targeted objective:

$$\max_{U_i} \int_0^{+\infty} \sum_{i=1}^{n} P_i(X_i, U_i) e^{-\rho t} dt \tag{11}$$

s.t. (4)

We use Pontryagin's maximum principle [Pontryagin et al., 1964] to solve this problem and therefore define the current value Hamiltonian given the shadow price vector $\lambda = (\lambda_i)_{i\in\{1,\dots,n\}}$ for pollution.

The Hamiltonian is expressed as:

$$\begin{aligned} \mathscr{H}_P(X, U, \lambda) = &\sum_{i=1}^{n} P_i(X_i, U_i) \\ &+ \sum_{i=1}^{n} \lambda_i \left[U_i - S_i X_i + V_i \frac{X_i^{\alpha_i}}{1 + X_i^{\alpha_i}} + \sum_{j\neq i} \Delta_{ij}(Z_{ij} X_j - X_i) \right] \end{aligned} \tag{12}$$

The necessary conditions for optimality are (see also sufficiency conditions in appendix 6.4.1):

$$\frac{\partial \mathscr{H}_P(X, U, \lambda)}{\partial U} = 0 \Leftrightarrow \forall i, \frac{\partial P_i(X_i, U_i)}{\partial U_i} = -\lambda_i \tag{13}$$

$$\frac{d\lambda}{d\tau} = \rho\lambda - \frac{\partial \mathscr{H}_P(X,U,\lambda)}{\partial X} \Leftrightarrow$$
$$\forall i, \frac{d\lambda_i}{d\tau} = \rho\lambda_i - \frac{\partial P_i(X_i,U_i)}{\partial X_i} + \lambda_i \left[S_i - V_i \frac{\alpha_i X_i^{(\alpha_i-1)}}{(1+X_i^{\alpha_i})^2} + \sum_{j\neq i} \Delta_{ij} \right] \tag{14}$$
$$- \sum_{j\neq i} \lambda_j \Delta_{ji} Z_{ji}$$

$$\frac{dX_i}{d\tau} = \frac{\partial \mathscr{H}_P(X,U,\lambda)}{\partial \lambda} \Leftrightarrow$$
$$\forall i, \frac{dX_i}{d\tau} = U_i - S_i X_i + V_i \frac{X_i^{\alpha_i}}{1+X_i^{\alpha_i}} + \sum_{j\neq i} \Delta_{ij}(Z_{ij}X_j - X_i). \tag{15}$$

Differentiating equation (13) with regard to τ and assuming that $\frac{\partial^2 P_i(X_i,U_i)}{\partial U_i \partial X_i} = 0$ we obtain:

$$\forall i, \frac{d\lambda_i}{d\tau} = -\frac{\partial^2 P_i(X_i,U_i)}{\partial U_i^2} \frac{dU_i}{d\tau} \tag{16}$$

Now we can replace λ in equation (14) and obtain the optimal dynamic equation for pollution loading:

$$\begin{aligned} \frac{dU_i}{d\tau} =& \frac{\frac{\partial P_i(X_i,U_i)}{\partial U_i}}{\frac{\partial^2 P_i(X_i,U_i)}{\partial U_i^2}} \left(\rho + \frac{\frac{\partial P_i(X_i,U_i)}{\partial X_i}}{\frac{\partial P_i(X_i,U_i)}{\partial U_i}} + S_i - V_i \frac{\alpha_i X_i^{(\alpha_i-1)}}{(1+X_i^{\alpha_i})^2} \right) \\ &+ \frac{\frac{\partial P_i(X_i,U_i)}{\partial U_i}}{\frac{\partial^2 P_i(X_i,U_i)}{\partial U_i^2}} \left(\sum_{j\neq i} \Delta_{ij} + \sum_{j\neq i} \frac{\frac{\partial P_j(X_j,U_j)}{\partial U_j}}{\frac{\partial P_i(X_i,U_i)}{\partial U_i}} \Delta_{ji} Z_{ji} \right) \end{aligned} \tag{17}$$

For all i and j, let the marginal rate of utility substitution between pollution stock

and pollution loading be $MRS_{X_iU_i}$ and denote as $MRS_{U_jU_i}$ the marginal rate of utility substitution between pollution loading in plot j and pollution loading in plot i. Furthermore let R_{A_i} denote the rate of absolute risk aversion of the utility function P_i.

$$MRS_{X_iU_i} = -\frac{\frac{\partial P_i(X_i,U_i)}{\partial X_i}}{\frac{\partial P_i(X_i,U_i)}{\partial U_i}}; MRS_{U_jU_i} = -\frac{\frac{\partial P_j(X_j,U_j)}{\partial U_j}}{\frac{\partial P_i(X_i,U_i)}{\partial U_i}}; R_{A_i} = -\frac{\frac{\partial P_i(X_i,U_i)}{\partial U_i}}{\frac{\partial^2 P_i(X_i,U_i)}{\partial U_i^2}} \tag{18}$$

We obtain

$$\begin{aligned}\frac{dU_i}{d\tau} =& - R_{A_i}\left(\rho - MRS_{X_iU_i} + S_i - V_i\frac{\alpha_i X_i^{(\alpha_i-1)}}{(1+X_i^{\alpha_i})^2}\right) \\ & - R_{A_i}\left(\sum_{j\neq i}\Delta_{ij} - \sum_{j\neq i} MRS_{U_jU_i}\Delta_{ji}Z_{ji}\right).\end{aligned} \tag{19}$$

In equation 19, the term $-R_{A_i}\left(\sum_{j\neq i}\Delta_{ij} - \sum_{j\neq i} MRS_{U_jU_i}\Delta_{ji}Z_{ji}\right)$ represents the impact of the system's spatial connectivity on the optimal dynamics of the control U_i.

Provided $R_{A_i} \neq 0$ this means that the curve representing potential equilibrium levels of pollution stock will always be lower with dispersion compared to without because $\sum_{j\neq i}\Delta_{ij} - \sum_{j\neq i} MRS_{U_jU_i}\Delta_{ji}Z_{ji} > 0$. This is the case because $MRS_{U_jU_i} < 0, \forall i$ and j. This difference is linearly increasing with the rate of dispersion in both directions, the difference in pollution thresholds between plot i and other plots and the marginal rate of utility substitution between pollution loading in plot j and pollution loading in plot i.

Following Wagener [2003], we illustrate this result in a simple case where $\forall i$, $P_i(X_i, U_i) = \ln U_i - \eta X_i^2$. In this case $MRS_{X_iU_i} = -2\eta X_i U_i$, $MRS_{U_jU_i} = -\frac{U_i}{U_j}$ and $R_{A_i} = U_i$. This gives the equation for optimal pollution control dynamics:

$$\frac{dU_i}{d\tau} = -U_i \left(\rho + 2\eta X_i U_i + S_i - V_i \frac{\alpha_i X_i^{(\alpha_i - 1)}}{(1 + X_i^{\alpha_i})^2} + \sum_{j \neq i} \Delta_{ij} + \sum_{j \neq i} \frac{U_i}{U_j} \Delta_{ji} Z_{ji} \right). \quad (20)$$

We now plot the phase diagram for this problem (figure 3), which we obtain by plotting the curves of $\frac{dX_i}{d\tau} = \frac{dU_i}{d\tau} = 0$, which correspond to the conditions

$$\begin{aligned} U_i &= S_i X_i - V_i \frac{X_i^{\alpha_i}}{1 + X_i^{\alpha_i}} - \sum_{j \neq i} \Delta_{ij} (Z_{ij} X_j - X_i) \\ U_i &= \frac{-1}{2\eta X_i + \sum_{j \neq i} \frac{\Delta_{ji} Z_{ji}}{U_j}} \left(\rho + S_i - V_i \frac{\alpha_i X_i^{(\alpha_i - 1)}}{(1 + X_i^{\alpha_i})^2} + \sum_{j \neq i} \Delta_{ij} \right). \end{aligned} \quad (21)$$

Figure 3 illustrates the impacts of dispersion on an optimally controlled system. Here the system without dispersion, corresponds to case (iv) in figure 4 of Wagener [2003]. Two interior equilibria exist and the low pollution equilibrium is reached for initial conditions below an indifference (Skiba) point, while the high pollution equilibrium is reached for initial conditions above the Skiba point. The outcome in the system with dispersion will then depend also on the equilibrium status in the other plots. If the equilibrium pollution stock in other plots is low, at an equilibrium similar to the low pollution equilibrium in plot i the system with dispersion will only have one low pollution equilibrium. The possibility of a skiba point and alternate high pollution equilibrium disappears in that case (3a).

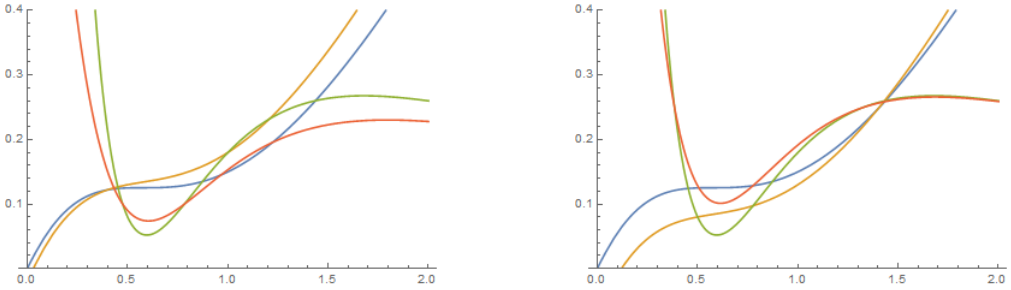

(a) $X_j = 0.4$; $U_j = 0.1$ (b) $X_j = 1.4$; $U_j = 0.25$

Figure 3: Projection of the phase diagrams of the controlled pollution system in (X_i, U_i)-space assuming (X_j, U_j) represent all other patches lumped and in equilibrium. Pollution dynamics with (orange) and without dispersion (blue) and control dynamics with (red) and without dispersion (green). In both figures, the case with no dispersion corresponds to case (iv) in Figure 4 of Wagener [2003], where two alternate equilibria are possible and a Skiba point exists. (a) The equilibrium in plot j is at approximately the same level as the low pollution equilibrium in plot i. Only the low equilibrium remains with dispersion. (b) The equilibrium in plot j is at approximately the same level as the high pollution equilibrium in plot i. Only the high equilibrium level remains with dispersion. Figures drawn using Mathematica. $S_i = 0.65$; $V_i = 1$; $\alpha_i = 2$; $\rho = 0.03$; $\eta = 0.5$; $Z_{ij} = 0.6$ $\sum_{j \neq i} \Delta_{ij} = 0.05$.

However if the stock in other plots is relatively high, mimicked by an equilibrium stock in plot j at approximately the same level as the high pollution equilibrium in plot i, then only a high pollution equilibrium is possible in plot i (3b).

4.2 Controlling resource cascades

Let $\Omega_i(Y_i, H_i)$ denote the the time varying instantaneous objective in each resource patch i, where Y_i and H_i, respectively, denote the vectors of resource stocks $(Y_i)_{i\in\{1,\dots,n\}}$ respectively harvest $(H_i)_{i\in\{1,\dots,n\}}$.

We can formulate a manager's resource management problem as:

$$\max_{H_i} \int_0^{+\infty} \sum_{i=1}^{n} \Omega_i(Y_i, H_i) e^{-\rho t} dt \tag{22}$$

s.t.:

$$\frac{dY_i}{d\tau} = R_i Y_i \left(1 - \frac{Y_i}{K_i}\right) - C_i \frac{Y_i^{\beta_i}}{1 + Y_i^{\beta_i}} - H_i + \sum_{j\neq i} D_{ij}(Q_{ij} Y_j - Y_i) \tag{23}$$

We use Pontryagin's maximum principle to solve this problem and therefore define the current value Hamiltonian given the shadow price vector $\mu = (\mu_i)_{i\in\{1,\dots,n\}}$ for resource dynamic constraints in all the patches. The Hamiltonian is expressed as:

$$\begin{aligned}\mathscr{H}_R(Y, H, \mu) = &\sum_{i=1}^{n} \Omega_i(Y_i, H_i) \\ &+ \sum_{i=1}^{n} \mu_i \left[R_i Y_i \left(1 - \frac{Y_i}{K_i}\right) - C_i \frac{Y_i^{\beta_i}}{1 + Y_i^{\beta_i}} - H_i + \sum_{j\neq i} D_{ij}(Q_{ij} Y_j - Y_i) \right]\end{aligned} \tag{24}$$

The necessary conditions for optimality are (see also appendix 6.4.2 for the sufficiency conditions):

$$\frac{\partial \mathscr{H}_R(Y,H,\mu)}{\partial H} = 0 \Leftrightarrow \forall i, \frac{\partial \Omega_i(Y_i,H_i)}{\partial H_i} = \mu_i \tag{25}$$

$$\begin{aligned}
&\frac{d\mu}{d\tau} = \rho\mu - \frac{\partial \mathscr{H}_R(Y,H,\mu)}{\partial Y} \Leftrightarrow \\
&\quad \forall i, \frac{d\mu_i}{d\tau} = \rho\mu_i - \frac{\partial \Omega_i(Y_i,H_i)}{\partial Y_i} - \mu_i \left[R_i \left(1 - \frac{2Y_i}{K_i}\right) - C_i \frac{\beta_i Y_i^{(\beta_i - 1)}}{\left(1 + Y_i^{\beta_i}\right)^2} - \sum_{j \neq i} D_{ij} \right] \\
&\quad - \sum_{j \neq i} \mu_j D_{ji} Q_{ji}
\end{aligned} \tag{26}$$

$$\begin{aligned}
&\frac{dY_i}{d\tau} = \frac{\partial \mathscr{H}_R(Y,H,\mu)}{\partial \mu} \\
&\Leftrightarrow \forall i, \frac{dY_i}{d\tau} = R_i Y_i \left(1 - \frac{Y_i}{K_i}\right) - C_i \frac{Y_i^{\beta_i}}{1 + Y_i^{\beta_i}} - H_i + \sum_{j \neq i} D_{ij}(Q_{ij} Y_j - Y_i)
\end{aligned} \tag{27}$$

Differentiating equation (25) with regard to τ and assuming that $\frac{\partial^2 \Omega_i(Y_i,H_i)}{\partial H_i \partial Y_i} = 0$, we obtain:

$$\forall i, \frac{d\mu_i}{d\tau} = \frac{\partial^2 \Omega_i(Y_i,H_i)}{\partial H_i^2} \frac{dH_i}{d\tau} \tag{28}$$

Now we can replace μ in equation (26) and obtain the optimal dynamic equation for harvest:

$$\frac{\partial^2\Omega_i(Y_i,H_i)}{\partial H_i^2}\frac{dH_i}{d\tau} = \rho\frac{\partial\Omega_i(Y_i,H_i)}{\partial H_i} - \frac{\partial\Omega_i(Y_i,H_i)}{\partial Y_i} - \frac{\partial\Omega_i(Y_i,H_i)}{\partial H_i}\left[R_i\left(1-\frac{2Y_i}{K_i}\right) - C_i\frac{\beta_i Y_i^{(\beta_i-1)}}{\left(1+Y_i^{\beta_i}\right)^2} - \sum_{j\neq i} D_{ij}\right] - \sum_{j\neq i}\frac{\partial\Omega_j(Y_j,H_j)}{\partial H_j}D_{ji}Q_{ji} \tag{29}$$

For all i and j and assuming that $\frac{\partial\Omega_i(Y_i,H_i)}{\partial H_i} \neq 0$ and $\frac{\partial^2\Omega_i(Y_i,H_i)}{\partial H_i^2} \neq 0$, let the marginal rate of utility substitution between resource stock and harvest be $MRS_{Y_iH_i}$ and denote as $MRS_{H_jH_i}$ the marginal rate of utility substitution between harvest in plot j and harvest in plot i. Furthermore let $\mathbb{R}_{A_i}$ denote the rate of absolute risk aversion of the utility function Ω_i.

$$MRS_{Y_iH_i} = -\frac{\frac{\partial\Omega_i(Y_i,H_i)}{\partial Y_i}}{\frac{\partial\Omega_i(Y_i,H_i)}{\partial H_i}}; MRS_{H_jH_i} = -\frac{\frac{\partial\Omega_j(Y_j,H_j)}{\partial H_j}}{\frac{\partial\Omega_i(Y_i,H_i)}{\partial H_i}}; \mathbb{R}_{A_i} = -\frac{\frac{\partial\Omega_i(Y_i,H_i)}{\partial H_i}}{\frac{\partial^2\Omega_i(Y_i,H_i)}{\partial H_i^2}} \tag{30}$$

We obtain

$$\frac{dH_i}{d\tau} = -\mathbb{R}_{A_i}\left(\rho + MRS_{Y_iH_i} - R_i\left(1-\frac{2Y_i}{K_i}\right) + C_i\frac{\beta_i Y_i^{(\beta_i-1)}}{\left(1+Y_i^{\beta_i}\right)^2}\right) - \mathbb{R}_{A_i}\left(\sum_{j\neq i} D_{ij} + \sum_{j\neq i} MRS_{H_jH_i}D_{ji}Q_{ji}\right) \tag{31}$$

In equation 31, the term $-\mathbb{R}_{A_i}\left(\sum_{j\neq i} D_{ij} + \sum_{j\neq i} MRS_{H_jH_i} D_{ji} Q_{ji}\right)$ represents the impact of the system's spatial connectivity on the optimal dynamics of the control H_i. This terms represents the trade off between the impact of the outflow from patch i (i.e. $\sum_{j\neq i} D_{ij}$) on the harvest in that patch and the impact of harvests in other patches on the inflow to patch i, represented by the marginal rate of substitution between harvesting in plot i and all the other plots. If the marginal impact on the objective of harvesting in other plots is relatively large compared to the marginal impact of harvesting in plot i, then the marginal rate of substitution will be large compared to the outflow from patch i and the equilibrium harvest curve for plot i could be lower with connectivity than without.

In a similar way as in section 4.1, we illustrate this result in a simple case where $\forall i$, $\Omega_i(Y_i, H_i) = \ln H_i - \frac{\theta}{Y_i}$, where θ_i denotes the unit cost of fishing effort per catchability unit.[3] In this case $MRS_{Y_iH_i} = -\frac{\theta H_i}{Y_i^2}$, $MRS_{H_jH_i} = -\frac{\pi_i}{\pi_j}$ and $R_{A_i} = -H_i$. This gives the equation for optimal harvest dynamics:

$$\begin{aligned}\frac{dH_i}{d\tau} = H_i &\left(\rho - \frac{\theta H_i}{Y_i^2} - R_i\left(1 - \frac{2Y_i}{K_i}\right) + C_i \frac{\beta_i Y_i^{(\beta_i - 1)}}{\left(1 + Y_i^{\beta_i}\right)^2}\right) \\ &+ H_i\left(\sum_{j\neq i} D_{ij} - \sum_{j\neq i} \frac{H_i}{H_j} D_{ji} Q_{ji}\right)\end{aligned} \tag{32}$$

We now plot the phase diagram for this problem (figure 4, which we obtain by

[3] In Munro and Sumaila [2015] this is denoted by b/q, where b is the unit cost of fishing effort and q the catchability coefficient.

plotting the curves of $\frac{dY_i}{d\tau} = \frac{dH_i}{d\tau} = 0$, which correspond to the conditions

$$\begin{aligned} H_i &= R_i Y_i \left(1 - \frac{Y_i}{K_i}\right) - C_i \frac{Y_i^{\beta_i}}{1 + Y_i^{\beta_i}} + \sum_{j \neq i} D_{ij}(Q_{ij} Y_j - Y_i) \\ H_i &= \frac{1}{\frac{Y_i^2}{\theta} + \sum_{j \neq i} \frac{D_{ji} Q_{ji}}{H_j}} \left(\rho - R_i \left(1 - \frac{2Y_i}{K_i}\right) + C_i \frac{\beta_i Y_i^{(\beta_i - 1)}}{\left(1 + Y_i^{\beta_i}\right)^2} + \sum_{j \neq i} D_{ij} \right). \end{aligned} \tag{33}$$

Figure 4 illustrates six possible outcomes of controlling a resource stock with and without dispersion in a focal patch i, depending on the size of stocks and harvests in other plots and the influence of predation. We investigate situations when the other plot has approximately the same conditions (equilibrium stock and harvest) as the focal plot without dispersion in high resource equilibrium (figures 4a, 4c, 4e) alternatively in low resource equilibrium (figures 4b, 4d, 4f). The influence of predation is either low (figures 4a, 4b), intermediate (figures 4c, 4d), or high (figures 4e, 4f). We find that dispersion either leads to lower stock growth overall (figures 4b, 4c, and 4f) or to higher growth over all (figures 4d and 4e) or can increase growth at low stock levels and decrease growth at high stock levels (figure 4a). However this property is not linearly correlated with the size of the stocks in the other plots as high stock levels in other plots can lead to either cases (figures 4a, 4c, 4e) and low stock levels in other plots can at least lead to either higher growth (Figure 4d) or lower growth (figures 4b, and 4f).

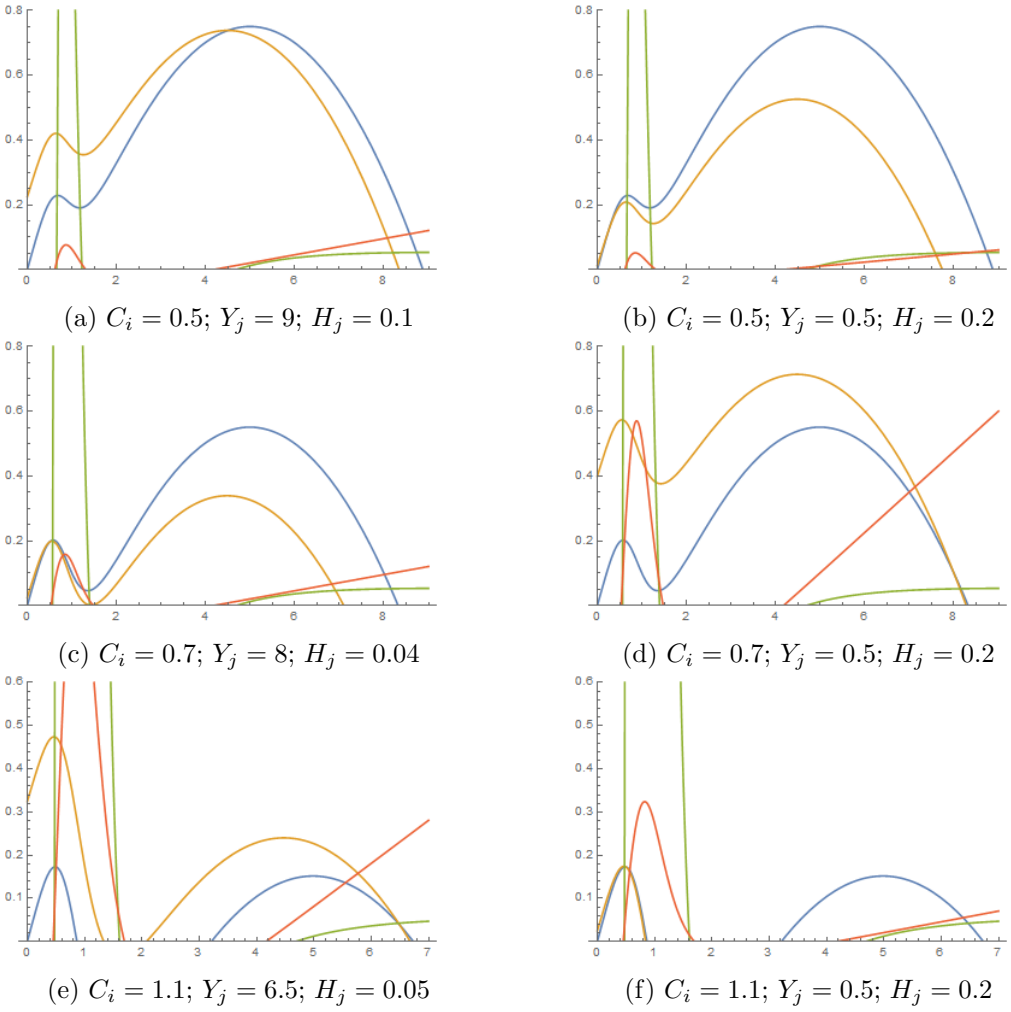

(a) $C_i = 0.5$; $Y_j = 9$; $H_j = 0.1$

(b) $C_i = 0.5$; $Y_j = 0.5$; $H_j = 0.2$

(c) $C_i = 0.7$; $Y_j = 8$; $H_j = 0.04$

(d) $C_i = 0.7$; $Y_j = 0.5$; $H_j = 0.2$

(e) $C_i = 1.1$; $Y_j = 6.5$; $H_j = 0.05$

(f) $C_i = 1.1$; $Y_j = 0.5$; $H_j = 0.2$

Figure 4: Projection of the phase diagrams of the controlled resource system in (Y_i, H_i)-space assuming (Y_j, H_j) represent all other patches lumped and in equilibrium. Resource dynamics with (orange) and without dispersion (blue) and control (harvest) dynamics with (red) and without dispersion (green). The instantaneous objective function is $\Omega_i(Y_i, H_i) = \ln H_i - \frac{\theta}{Y_i}$. Equilibria in plot j are at similar level as the high stock equilibrium in plot i (a, c, and e). Equilibria in plot j are at similar level as the low stock equilibrium in plot i (b, d, and f). Predation is limited (a, b); intermediate (c, d) or high (e, f). $R_i = 0.5$; $K_i = 10$; $\beta_i = 4$; $\rho = 0,03$; $\theta = 0.1$; $Z_{ij} = 1$; $\sum_{j \neq i} D_{ij} = 0.05$. Figures drawn using Mathematica.

5 Concluding discussion

We built a modelling framework to analyse the impacts of dispersion on the provision of ecosystem services, in particular pollution absorption and resource reproduction, in ecosystems that can undergo a regime shift. We modelled pollution as an inflow of pollution (which can be controlled) to the system, an internal deposition, and an internal release of pollution above a threshold. The ecosystem producing a renewable resource is modelled using a logistic growth function, and a convex-concave predation term and a harvest term representing resource control. In both types of systems, we model dispersion as flows between patches that can occur in both directions and at different rates between each pair of connected patches. We show that the impact of type of dispersion in a particular system (patch) depends on the rate of dispersion between connected patches and the threshold differential between these patches.

Examination of the impacts of dispersion in non-controlled systems illustrates the potentially substantial effects of dispersion in these systems. Not only can dispersion influence the location of potential equilibria, it can also influence their numbers. This is true for both types of systems. In particular, we show that for pollution systems, dispersion implies that the net inflow to the system is always lower at low stock values but increases more steeply with increases in stock with dispersion compared to without dispersion. For resource systems we can identify conditions under which the resource growth is higher with dispersion than without. This occurs when the total inflow from other plots and the net growth of the stock are relatively large compared to the intrinsic growth rate. If they instead are relatively small, then dispersion will lead to a lower resource growth in the plot.

We also solved the problem of a planner who want to optimally control their pollution or resource system. In both cases we could derive necessary conditions for an optimal outcome consisting of the dynamic state equation and a dynamic control equation. We find in both cases that the dynamic control equation with dispersion and regime shifts contains two additional terms compared to the corresponding equations without dispersion and regime shifts. One term shows the impact of potential regime shifts in the optimal control and goes in the opposite direction of the other terms in both cases. One term shows the impact of dispersion on the control, which consists of the net inflow to the typical patch. Its direction will depend on whether the outflow is larger than the inflow or not. If the outflow is higher than the inflow, the regime shift effect is reinforced, while it is counteracted if it is lower.

We illustrate how controlling a pollution system without incorporating system dispersion can lead to completely erroneous advice. Depending on the status of the patches connected to the observed patch, dispersion could lead to different outcomes concerning the number and location of possible steady states compared to the solution without dispersion. For a system without dispersion that exhibits an indifference threshold, we show that the pollution stock and control in the connected system can actually result in a unique low pollution level if the connected patch had a low pollution equilibrium or a unique high pollution level if the connected patch had a high pollution equilibrium. It remains to investigate whether intermediate cases with indifference thresholds are possible, when the focal plot is in such situation without dispersion. This is likely at least when the influence of other patches is marginal. Further parameter sensitivity analysis is likely to throw

some light on this issue. We also illustrate multiple ways in which dispersion could alter the number of equilibria compared to a situation with no dispersion.

Here we have only investigated connections between similar types of systems. However Rocha et al. [2018] find evidence that different types of systems can also trigger cascading regime shifts through their connection. For example pollution leading to climate change or some other resource could influence resource growth, their carrying capacity, and or shelter against predation and thereby generate cascading shifts. In the other way around, some ecosystem resources could also influence the level of pollution in another system, for example through some inflow of nutrients perhaps due to substantial death events (e.g. algae blooms and coastal death zones).

In our study we controlled pollution and resources directly through pollution inflow and resource harvest. However, given that dispersion seems to have the potential to substantially alter system dynamics, it could be valuable to also investigate the opportunities and impacts of controlling system connections. For example responses to pandemic diseases include control of connectivity between people through the limitations of travels across countries and even within smaller communities through lock-downs. The same is true for invasive species. Hence future research could use our framework for a more systematic investigation of the impacts of controlling connectivity on the propensity to trigger or hinder regime shifts to spread between connected systems.

Finally it is likely to be fruitful to investigate the dynamics of whole systems of linked patches rather than just focusing on how one typical patch is influenced by other connected patches. In doing so we would need to investigate the implication

of the topology of the network of patches, in addition to just looking at the direction and size of the connections between connected patches. Just like Wilen [2007] and Rocha et al. [2015] have shown earlier, it is likely that the outcome may change depending on which plots are connected to each other and how.

It is clear already from the results of this paper that ignoring spatial dynamics can generate erroneous predictions and substantially flawed policy in contexts where connected systems can shift between alternate regimes. Based on these results it becomes important to investigate how much dispersion can fundamentally change a system's dynamics. This is likely to depend on the kind of systems studied. For some systems we may already be able to find answers since there is empirical evidence of cascading regime shifts [Rocha et al., 2018]. In other cases, a fundamental change in system dynamics might just be a mathematical curiosity that will never materialise in real life. However this paper suggests that it is time to systematically investigate and quantify the role of spatial heterogeneity in relation to regime shifts dynamics. This paper is a first stepping stone in that direction. It provides a useful framework for doing so, which builds on standard ways of modelling resource and pollution management, two essential ecosystem services contributions to the well-being of humanity.

6 Appendix

6.1 Types of regime shifts

Table 1 illustrates different types of regime shifts studied in the regime shift database and assesses whether they link to pollution (1), resource exploitation

(2), both (3) or none of them (4) in their triggers or consequences.

6.2 Simplification of the pollution system

Recall equation 3:

$$\frac{dx_i}{dt} = u_i - s_i x_i + v_i \frac{x_i^{\alpha_i}}{z_i^{\alpha_i} + x_i^{\alpha_i}} - \sum_{j \neq i} (\delta_{ij} x_i - \delta_{ji} x_j) \tag{34}$$

Let $X_i = \frac{x_i}{z_i}$ and choose the time scale of X_i so that $\frac{dt}{d\tau} = \frac{1}{r}$ then we obtain:

$$\begin{aligned} \frac{dX_i}{d\tau} = \frac{dX_i}{dx_i}\frac{dx_i}{dt}\frac{dt}{d\tau} =& \frac{1}{z_i}\frac{1}{r}\left(u_i - s_i z_i X_i + v_i \frac{(z_i X_i)^{\alpha_i}}{z_i^{\alpha_i} + (z_i X_i)^{\alpha_i}}\right) \\ & - \frac{1}{z_i}\frac{1}{r}\left(\sum_{j \neq i} (\delta_{ij} z_i X_i - \delta_{ji} z_j X_j)\right). \end{aligned} \tag{35}$$

Hence

$$\frac{dX_i}{d\tau} = \frac{u_i}{r z_i} - \frac{s_i}{r} X_i + \frac{v_i}{r z_i} \frac{X_i^{\alpha_i}}{1 + X_i^{\alpha_i}} - \sum_{j \neq i} \left(\frac{\delta_{ij}}{r} X_i - \frac{\delta_{ji} z_j}{r z_i} X_j\right). \tag{36}$$

Now let $U_i = \frac{u_i}{r z_i}$, $S_i = \frac{s_i}{r}$, $V_i = \frac{v_i}{r z_i}$, $Z_{ij} = \frac{\delta_{ji} z_j}{\delta_{ij} z_i}$ and $\Delta_{ij} = \frac{\delta_{ij}}{r}$, we obtain:

$$\frac{dX_i}{d\tau} = U_i - S_i X_i + V_i \frac{X_i^{\alpha_i}}{1 + X_i^{\alpha_i}} + \sum_{j \neq i} \Delta_{ij} (Z_{ij} X_j - X_i) \tag{37}$$

.

6.3 Simplification of the resource system

Recall equation 6:

$$\forall i \in \{1, ..., n\}, \frac{dy_i}{dt} = r_i y_i \left(1 - \frac{y_i}{k_i}\right) - c_i \frac{y_i^{\beta_i}}{q_i^{\beta_i} + y_i^{\beta_i}} - \sum_{j \neq i} (d_{ij} y_i - d_{ji} y_j). \tag{38}$$

Let $Y_i = \frac{y_i}{q_i}$ and choose the time scale of Y_i so that $\frac{dt}{d\tau} = \frac{1}{r}$ then we obtain:

$$\begin{aligned} \frac{dY_i}{d\tau} = \frac{dY_i}{dy_i}\frac{dy_i}{dt}\frac{dt}{d\tau} = &\frac{dY_i}{dy_i}\frac{1}{r}\left(r_i q_i Y_i \left(1 - \frac{q_i Y_i}{k_i}\right) - c_i \frac{(q_i Y_i)^{\beta_i}}{q_i^{\beta_i} + (q_i Y_i)^{\beta_i}}\right) \\ &\frac{dY_i}{dy_i}\frac{1}{r}\left(-\sum_{j \neq i} (d_{ij} q_i Y_i - d_{ji} q_j Y_j)\right). \end{aligned} \tag{39}$$

Hence

$$\frac{dY_i}{d\tau} = \frac{r_i}{r} Y_i \left(1 - \frac{q_i Y_i}{k_i}\right) - \frac{c_i}{r q_i} \frac{Y_i^{\beta_i}}{1 + Y_i^{\beta_i}} - \sum_{j \neq i} \left(\frac{d_{ij}}{r} Y_i - \frac{d_{ji} q_j}{q_i r} Y_j\right) \tag{40}$$

Now let $R_i = \frac{r_i}{r}$, $K_i = \frac{k_i}{q_i}$, $C_i = \frac{c_i}{r q_i}$, $Q_j = \frac{d_{ji} q_j}{d_{ij} q_i}$, and $D_{ij} = \frac{d_{ij}}{r}$. We obtain:

$$\frac{dY_i}{d\tau} = R_i Y_i \left(1 - \frac{Y_i}{K_i}\right) - C_i \frac{Y_i^{\beta_i}}{1 + Y_i^{\beta_i}} + \sum_{j \neq i} D_{ij} (Q_j Y_j - Y_i) \tag{41}$$

.

6.4 Sufficiency conditions

6.4.1 Pollution problems

Arrow's sufficiency condition states that the maximized current value Hamiltonian should be concave with regard to the vector of state variables X. Let $\hat{\mathscr{H}}_P(X, U, \lambda)$ denote the maximized current value Hamiltonian for the pollution problem and let U^* denote the optimal control, then the maximized current value Hamiltonian is expressed as:

$$\begin{aligned}\hat{\mathscr{H}}_P(X, U, \lambda) = &\sum_{i=1}^{n} P_i(X_i, U_i^*) \\ &+ \sum_{i=1}^{n} \lambda_i \left[U_i^* - S_i X_i + V_i \frac{X_i^{\alpha_i}}{1 + X_i^{\alpha_i}} + \sum_{j \neq i} \Delta_{ij}(Z_{ij} X_j - X_i) \right]\end{aligned} \tag{42}$$

Further let $M_r^P(X)$ denote the principal minor of order r in the Hessian for $\hat{\mathscr{H}}_P(X, U, \lambda)$. The maximized Hamiltonian is concave in X on $\mathbb{R}_+^n$ if and only if for all points $(X_1, ..., X_n)$ and for all $M_r^P(X)$, $(-1)^r M_r^P(X) \geq 0$ for $r \in [1, n]$. The Hessian matrix for $\hat{\mathscr{H}}_P(X, U, \lambda)$ is given by:

$$\begin{vmatrix} \frac{\partial^2 \hat{\mathscr{H}}_P(X,U,\lambda)}{\partial X_1^2} & \cdots & \frac{\partial^2 \hat{\mathscr{H}}_P(X,U,\lambda)}{\partial X_1 \partial X_j} & \cdots & \frac{\partial^2 \hat{\mathscr{H}}_P(X,U,\lambda)}{\partial x_1 \partial X_n} \\ \cdots & \cdots & \cdots & \cdots & \cdots \\ \frac{\partial^2 \hat{\mathscr{H}}_P(X,U,\lambda)}{\partial X_i \partial X_1} & \cdots & \frac{\partial^2 \hat{\mathscr{H}}_P(X,U,\lambda)}{\partial X_i \partial X_j} & \cdots & \frac{\partial^2 \hat{\mathscr{H}}_P(X,U,\lambda)}{\partial X_i \partial X_n} \\ \cdots & \cdots & \cdots & \cdots & \cdots \\ \frac{\partial^2 \hat{\mathscr{H}}_P(X,U,\lambda)}{\partial X_n \partial X_1} & \cdots & \frac{\partial^2 \hat{\mathscr{H}}_P(X,U,\lambda)}{\partial X_n \partial X_j} & \cdots & \frac{\partial^2 \hat{\mathscr{H}}_P(X,U,\lambda)}{\partial X_n^2} \end{vmatrix}$$

where $\forall i$ and $j \in [0, n]$, $\frac{\partial^2 \hat{\mathscr{H}}_P(X,U,\lambda)}{\partial X_i^2} = \frac{d^2 P_i(X_i,U_i)}{dX_i^2} + \lambda_i V_i \alpha_i (\alpha_i - 1) \frac{X_i^{(\alpha_i - 2)}}{(1 + X_i^{\alpha_i})^3}$ and $\frac{\partial^2 \hat{\mathscr{H}}_P(X,U,\lambda)}{\partial X_i \partial X_j} = 0$.

This corresponds to the series of conditions: $\forall r \in [1, n]$,
$(-1)^r \prod_{i=1}^{r} \left(\frac{d^2 P_i(X_i, U_i)}{dX_i^2} + \lambda_i V_i \alpha_i (\alpha_i - 1) \frac{X_i^{(\alpha_i - 2)}}{(1 + X_i^{\alpha_i})^3} \right) \geq 0.$

6.4.2 Resource problems

The sufficiency conditions are calculated in the same way for the resource problem and just like in the pollution problem the Hessian matrix is a matrix where only the diagonal terms are non zero.

References

J. M. Anderies, B. H. Walker, and A. P. Kinzig. Fifteen weddings and a funeral: case studies and resilience-based management. *Ecology and society*, 11(1), 2006.

R. Biggs, T. Blenckner, C. Folke, L. Gordon, A. Norstrom, M. Nystrom, and G. Peterson. Regime shifts,[in:] encyclopedia of theoretical ecology, a. *Hastings, LJ Gross,(ed), University of California Press, Berkeley*, pages 609–617, 2012a.

R. Biggs, M. Schlüter, D. Biggs, E. L. Bohensky, S. BurnSilver, G. Cundill, V. Dakos, T. M. Daw, L. S. Evans, K. Kotschy, et al. Toward principles for enhancing the resilience of ecosystem services. *Annual review of environment and resources*, 37:421–448, 2012b.

R. Biggs, M. Schlüter, and M. L. Schoon. *Principles for building resilience: sustaining ecosystem services in social-ecological systems*. Cambridge University Press, 2015.

W. Brock, A. Xepapadeas, et al. Spatial environmental and resource economics. Technical report, Athens University of Economics and Business, 2020.

W. A. Brock and D. Starrett. Managing systems with non-convex positive feedback. *Environmental and resource Economics*, 26(4):575–602, 2003.

C. D. Brummitt, G. Barnett, and R. M. D'Souza. Coupled catastrophes: sudden shifts cascade and hop among interdependent systems. *J. R. Soc. Interface*, 12 (112):20150712–20150712, Nov. 2015.

S. R. Carpenter, D. Ludwig, and W. A. Brock. Management of eutrophication for lakes subject to potentially irreversible change. *Ecological applications*, 9(3): 751–771, 1999.

A.-S. Crépin. *Tackling the economics of ecosystems*. PhD thesis, Stockholm University, 2002.

A.-S. Crépin. Multiple species boreal forests–what faustmann missed. *Environmental and Resource Economics*, 26(4):625–646, 2003.

A.-S. Crépin. Using fast and slow processes to manage resources with thresholds. *Environmental and Resource Economics*, 36(2):191–213, 2007.

A.-S. Crépin and E. Nævdal. Inertia risk: Improving economic models of catastrophes. *The Scandinavian Journal of Economics*, 2019.

A.-S. Crépin, R. Biggs, S. Polasky, M. Troell, and A. De Zeeuw. Regime shifts and management. *Ecological Economics*, 84:15–22, 2012.

M. M. Dekker, A. S. v. d. Heydt, and H. A. Dijkstra. Cascading transitions in the climate system. *Earth System Dynamics Discussions*, 9(4):1243–1260, 2018.

C. S. Holling. Some characteristics of simple types of predation and parasitism. *The Canadian Entomologist*, 91(7):385–398, 1959.

R. D. Horan, E. P. Fenichel, K. L. Drury, and D. M. Lodge. Managing ecological thresholds in coupled environmental–human systems. *Proceedings of the National Academy of Sciences*, 108(18):7333–7338, 2011.

V. Kaitala, M. Pohjola, and O. Tahvonen. Transboundary air pollution and soil acidification: A dynamic analysis of an acid rain game between finland and the ussr. *Environmental and Resource Economics*, 2(2):161–181, 1992.

A. P. Kinzig, P. Ryan, M. Etienne, H. Allison, T. Elmqvist, and B. H. Walker. Resilience and regime shifts: assessing cascading effects. *Ecology and society*, 11(1), 2006.

A. K. Klose, V. Karle, R. Winkelmann, and J. F. Donges. Emergence of cascading dynamics in interacting tipping elements of ecology and climate. *Royal Society open science*, 7(6):200599, 2020.

K. Kroetz and J. N. Sanchirico. The bioeconomics of spatial-dynamic systems in natural resource management. *Annu. Rev. Resour. Econ.*, 7(1):189–207, 2015.

J. Krönke, N. Wunderling, R. Winkelmann, A. Staal, B. Stumpf, O. A. Tuinenburg, and J. F. Donges. Dynamics of tipping cascades on complex networks. *arXiv preprint arXiv:1905.05476*, 2019.

C.-Z. Li, A.-S. Crépin, C. Folke, et al. The economics of resilience. *International Review of Environmental and Resource Economics*, 11(4):309–353, 2018.

K. Mäler. The acid rain game in: Folmer, h. and van ierland, e.(eds), valuation methods and policy making in environmental economics, 1989.

K.-G. Mäler and A. De Zeeuw. The acid rain differential game. *Environmental and Resource Economics*, 12(2):167–184, 1998.

K.-G. Mäler, A. Xepapadeas, and A. De Zeeuw. The economics of shallow lakes. *Environmental and resource Economics*, 26(4):603–624, 2003.

D. R. Mueller, P. Van Hove, D. Antoniades, M. O. Jeffries, and W. F. Vincent. High arctic lakes as sentinel ecosystems: Cascading regime shifts in climate, ice cover, and mixing. *Limnology and Oceanography*, 54(6part2):2371–2385, 2009.

G. R. Munro and U. R. Sumaila. On the contributions of colin clark to fisheries economics. *Environmental and Resource Economics*, 61(1):1–17, 2015.

J. Murray. *Mathematical biology II: spatial models and biomedical applications*. Springer New York, 2001.

Y. Nagase and E. C. Silva. Acid rain in china and japan: A game-theoretic analysis. *Regional Science and Urban Economics*, 37(1):100–120, 2007.

A. Okubo and S. A. Levin. *Diffusion and ecological problems: modern perspectives*, volume 14. Springer Science & Business Media, 2013.

D. P. Peters, O. E. Sala, C. D. Allen, A. Covich, and M. Brunson. Cascading events in linked ecological and socioeconomic systems. *Frontiers in Ecology and the Environment*, 5(4):221–224, 2007.

L. Pontryagin, V. Boltyanskii, R. Gamkrelidze, and E. Mischenko. *The Mathematical Theory of Optimal Processes, Translated by D.E. Brown*. Pergamon Press, 1964.

J. C. Rocha, G. D. Peterson, and R. Biggs. Regime shifts in the anthropocene: drivers, risks, and resilience. *PloS one*, 10(8), 2015.

J. C. Rocha, G. Peterson, Ö. Bodin, and S. Levin. Cascading regime shifts within and across scales. *Science*, 362(6421):1379–1383, 2018.

J. N. Sanchirico and J. E. Wilen. Bioeconomics of spatial exploitation in a patchy environment. *Journal of Environmental Economics and Management*, 37(2): 129–150, 1999.

M. D. Smith, J. N. Sanchirico, and J. E. Wilen. The economics of spatial-dynamic processes: applications to renewable resources. *Journal of Environmental Economics and Management*, 57(1):104–121, 2009.

P. F. Verhulst. Notice sur la loi que la population poursuit dans son accroissement. *Correspondance mathématique et physique*, 10:113–121, 1838.

F. O. Wagener. Skiba points and heteroclinic bifurcations, with applications to the shallow lake system. *Journal of economic dynamics and control*, 27(9): 1533–1561, 2003.

J. E. Wilen. Economics of spatial-dynamic processes. *American Journal of Agricultural Economics*, 89(5):1134–1144, 2007.

N. Wunderling, J. F. Donges, J. Kurths, and R. Winkelmann. Interacting tipping elements increase risk of climate domino effects under global warming. *Earth System Dynamics Discussions*, pages 1–21, 2020a.

N. Wunderling, A. Staal, B. Sakschewski, M. Hirota, O. Tuinenburg, J. Donges, H. Barbosa, and R. Winkelmann. Network dynamics of drought-induced tipping cascades in the amazon rainforest. *Researchsquare.com*, 2020b.

Regime shift	Type	Trigger or impact
Arctic Benthos Borealisation	4	Global warming
Arctic Sea-Ice Collapse	1	Global warming
Bivalves Collapse	3	Harvesting
Bush Encroachment	2	Grazing
Coastal Marine Eutrophication	1	Nutrient leackage
Common pool resource harvesting	1	Overexploitation
Coniferous to deciduous boreal forest	3	Fire frequency, which relates to forest harvest and global warming
Coral transitions	3	Nutrient leackage, warming and fishing
Fisheries collapse	3	Overexploitation
Forest to Savannahs	2	Grazing
Freswater eutrophication	1	Nutrient leackage
Greenland ice sheet collapse	1	Global warming
Hypoxia	1	Nutrient leackage
Indian Summer Monsoon	1	Global warming
Invasive floating to invasive submerged plant dominance	1	Nutrient leackage
Kelp transition	3	Harvest and Nutrient leackage
Mangrove transition	3	Global warming and impact on fish
Marine food webs: community change and trophic level decline	3	Harvest, global warming and upwelling
Peatland transition	1	Climate change and nutrient inputs
River Chanel position	4	Sediment build up and land clearance
Salt Marsh to Tidal Flat	1	Pollution by sedimentation
Seagrass transitions	3	Nutrient pollution
Soil Salinization	3	Pollution by salt and water as a resource
Sprawling vs Compact City	4	Urban expension and infrastructure
Steppe to Tundra	3	Climate change, nutrients, grazing
Submerged to floating plants	1	Nutrient and invasive species
Thermohaline circulation	1	Global warming
Thermokarst Lake to terrestrial ecosystem	1	Global warming which leads to melting permafrost
Tundra to Boreal Forest	3	Global warming and grazing
West Antarctic Ice Sheet collapse	1	Global warming

Table 1: Regime shifts types in the regime shift database (www.regimeshifts.org) and whether they relate to pollution (1), resource production (2), both (3) or none of those (4)

Name	Description	Type	Range
i and j	patch names, $j \neq i$	parameter	$\{1, ...n\}$
n	total number of patches	parameter	$\{1, ...\infty\}$
t	time step	variable	$[0, \infty]$
x_i	pollution stock in patch i	variable	$[0, ?]$
u_i	human load of pollution	parameter	$[0, ?]$
s_i	internal rate of loss	parameter	$[0, 1]$
v_i	maximum level of internal nutrient release	parameter	$[0, ?]$
z_i	pollution threshold	parameter	$[0, ?]$
α_i	sharpness of the shift between low and high pollution regimes	parameter	$[2, \infty]$
δ_{ij}	rate of pollution dispersion from patch i to j	parameter	[0,1]
$u_i - s_i x_i$	net inflow of pollution	function	$[0, \max\{x_i\}]$
$v_i \frac{x_i^{\alpha_i}}{z_i^{\alpha_i} + x_i^{\alpha_i}}$	internal release of pollution	function	$[0, v_i]$
$\sum_{j \neq i} \Delta_{ij} (x_j - x_i)$	pollution transports between patches i and j	function	[0,1]
y_i	resource stock in patch i	variable	[0,?]
r_i	intrinsic growth rate	parameter	[0,1?]
k_i	carrying capacity	parameter	$[0, \infty]$
c_i	maximum predation rate	parameter	[0,?]
q_i	pollution threshold	parameter	[0,?]
β_i	sharpness of the shift between low and high levels of predation	parameter	$[2, \infty]$
d_{ij}	rate of resource dispersion from patch i to j	parameter	[0,1]
$r_i y_i \left(1 - \frac{y_i}{k_i}\right)$	net inflow of pollution	function	$[0, \max\{y_i\}]$
$c_i \frac{y_i^{\beta_i}}{q_i^{\beta_i} + y_i^{\beta_i}}$	availability of refuges	function	$[0, c_i]$
$\sum_{j \neq i} d_{ij} (x_j - x_i)$	resource transport between patches i and j	function	[0,1]

Table 2: Names, description and range of the parameters, variables and functions used in the modelling framework

Name	Description	Type	Range
i and j	patch names, $j \neq i$	parameter	$\{1, ...n\}$
n	total number of patches	parameter	$\{1, ...\infty\}$
τ	time step	variable	$[0, \infty]$
r	time step difference	parameter	$[0, ...?]$
X_i	pollution stock in patch i	variable	[0,?]
U_i	human load of pollution	parameter	[0,?]
S_i	internal rate of loss	parameter	[0,1]
V_i	maximum internal nutrient release	parameter	[0,?]
Z_i	pollution threshold	parameter	[0,?]
α_i	sharpness of the shift	parameter	$[2, \infty]$
Δ_{ij}	rate of pollution dispersion from patch i to j	parameter	[0,1]
$U_i - X_i$	net inflow of pollution	function	$[0, \max\{X_i\}]$
$V_i \frac{X_i^{\alpha_i}}{1+X_i^{\alpha_i}}$	internal release of pollution	function	$[0, V_i]$
$\sum_j \neq i\Delta_{ij} (Z_j X_j - X_i)$	pollution transport between patches i and j	function	$[0, 1]$
Y_i	resource stock in patch i	variable	[0,?]
R_i	intrinsic growth rate	parameter	[0,1?]
K_i	carrying capacity	parameter	$[0, \infty]$
C_i	maximum predation rate	parameter	[0,?]
Q_j	pollution threshold	parameter	[0,?]
β_i	sharpness of the shift	parameter	$[2, \infty]$
D_{ij}	rate of resource dispersion from patch i to j	parameter	[0,1]
$R_i Y_i \left(1 - \frac{Y_i}{K_i}\right)$	net resource growth	function	$[0, \max\{Y_i\}]$
$C_i \frac{Y_i^{\beta_i}}{1+y_i^{\beta_i}}$	availability of refuges	function	$[0, C_i]$
$\sum_{j \neq i} D_{ij} (Q_j X_j - X_i)$	resource transport between patches i and j	function	$[0, 1]$

Table 3: Names, description and range of the parameters, variables and functions used in the normalised modelling framework. $X_i = \frac{x_i}{z_i}$, $\frac{dt}{d\tau} = \frac{1}{s_i}$, $U_i = \frac{u_i}{s_i z_i}$, $V_i = \frac{v_i}{s_i z_i}$, $Z_j = \frac{z_j}{z_i}$ and $\Delta_{ij} = \frac{\delta_{ij}}{s_i}$